Excited states of Nb_3N_2 and Nb_3C_2: Density functional theory, CASSCF, and MRCI studies

Matthew A. Addicoat and Gregory F. Metha[a)]
Department of Chemistry, University of Adelaide, Adelaide, South Australia 5005, Australia

(Received 18 December 2008; accepted 1 April 2009; published online 27 April 2009)

Complete active space self-consistent field (CASSCF) and multireference configuration interaction (MRCI) methods are used to investigate the Nb_3N_2 and Nb_3C_2 clusters in order to determine the agreement between multireference methods, density functional theory (DFT), and experiment. These two clusters are ideal candidates to study as the known spectroscopy can serve to validate the computational results, yet there is still room for the calculations to inform further spectroscopic experiments. We find that the MRCI leading configuration for each of the ground states is in agreement with that predicted by DFT but only accounts for up to 70% of the total configuration. CASSCF and DFT geometries are also in general agreement. Transition energies between the neutral and cationic manifolds are found to be poorly predicted by MRCI relative to the computationally cheap DFT method. For Nb_3C_2 we find that a higher energy isomer may have an electronic transition in the spectral vicinity as the lowest energy isomer. © *2009 American Institute of Physics*. [DOI: 10.1063/1.3122542]

I. INTRODUCTION

Transition metal clusters are characterized by a high density of states, which hampers both spectroscopic and computational elucidation of their electronic and geometric structures. Yet, it is the density of quantized states that gives them their interesting, and potentially useful, chemical and physical properties. Computationally, the high density of states suggests that multireference techniques would be necessary for accurate determination of cluster properties. However, the large number of electrons that need to be treated, coupled with their high spatial angular momentum (valence *d* electrons), and often, the high-spin state of the cluster, means that even the smallest of clusters are challenging and expensive to model. Consequently, very few transition metal clusters (defined here as having three or more transition metal atoms) have been examined using multireference methods. Those that have been investigated include Nb_{3-5},[1–3] Ru_3,[4] Rh_3,[5,6] Pd_3,[7] and Ag_3.[8] Similarly, there is also a dearth of high-level studies on the reaction products of metal clusters with molecules such as hydrides, carbides, nitrides, or oxides, although some diatomic species, such as NbC, have been investigated.

This lack of computational attention may be partly attributed to the fact that there is very little experimental spectroscopic information known about isolated metal clusters (i.e., in the gas phase). For the same reasons that these species are difficult to treat computationally, the high density of states makes experiments very difficult. Most success has come about from utilizing transitions between the respective ground electronic of different charge manifolds (i.e., anion → neutral and neutral → cation) because the ground states are relatively unperturbed and hence are analyzable.

A series of studies by workers at the Canadian National Research Council used pulsed-field ionization zero electron kinetic energy (ZEKE) spectroscopy to record vibrationally resolved spectra of species such as Nb_3C_2, Nb_5C_2, Y_3C_2, Nb_3N_2, Nb_3O, and Zr_3O.[9–11] Comparisons between the observed vibronic structure and that predicted theoretically from density functional theory (DFT)-optimized structures (for both the neutral and cation) using multidimensional Franck–Condon factors allowed geometries to be determined. For Nb_3N_2, a band origin with a short vibrational progression indicated little geometry change upon ionization. Their results suggested doubly bridging structures [shown in Fig. 1(a)] with C_{2v} symmetry for both the neutral (doublet) and cation (singlet). For Nb_3C_2, a much richer spectrum is observed starting at the origin and featuring a strong progression and six weaker ones. The density functional theory (DFT) results proposed two possible structures having doubly bridged (DB) or triply bridged (TB) carbon atoms [Figs. 1(a) and 1(b), respectively]. Their DFT calculations suggested that these structures were near-degenerate in the neutral species, however, in the cationic species the trigonal bipyramid structure (i.e., TB) was almost 1 eV lower in energy. On this basis and by employing simulated spectra they suggest a C_{2v} neutral (doublet) and a D_{3h} cation (singlet), both of TB geometry.

This paper reports our theoretical investigations into the electronic structures of neutral and cationic Nb_3C_2 and Nb_3N_2 using DFT, complete active space self-consistent field (CASSCF), and multireference configuration interaction (MRCI) methods and has several goals. First, to determine whether a more thorough theoretical investigation agrees with the observed spectroscopic assignment. Second, to determine the extent of multireference character in the ground

[a)]Author to whom correspondence should be addressed. Electronic mail: greg.metha@adelaide.edu.au. Tel.: +61 8 8303 5943. FAX: +61 8 8303 4358.

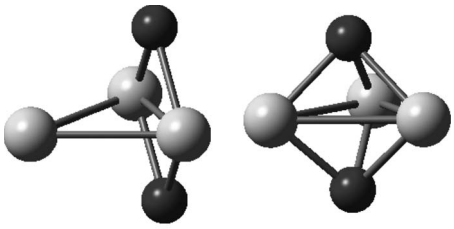

FIG. 1. DB and TB Nb_3X_2 structures. In both structures, the unique niobium atom (Nb′) is the leftmost atom. A typical $\phi_{Nb'NbNbX}$ is 75°–95° for DB structures and 60°–75° for TB structures.

states of these species. Finally, to calculate the low-lying excited states of these species, with a view to determining whether future experimental investigations could reveal excited states of these interesting metal cluster species.

II. COMPUTATIONAL METHOD

DFT calculations were undertaken using GAUSSIAN03 (Ref. 12) and employed the B3LYP (Ref. 13) functional with the Stuttgart (srsc) basis set and associated effective core potentials (ECPs) for niobium atoms and D95V (Ref. 14) for carbon and nitrogen atoms. All calculations were performed within the C_{2v} point group. Geometries of each electronic symmetry up to and including octet $(2S+1=8)$ states (septet in the case of cationic species) were optimized and frequency calculations were subsequently undertaken.

Similarly, full geometry optimizations (in C_{2v} symmetry) of each electronic state up to the octet were undertaken at the CASSCF level using the Werner–Meyer–Knowles[15,16] technique in MOLPRO-2006. Single point MRCI and MRCI+Q (Refs. 17 and 18) calculations were undertaken on all states of the lowest two multiplicities for both the neutral and cationic species (i.e., neutral doublets and quartets and cationic singlets and triplets). These calculations included up to 125×10^6 configurations; all CASSCF configurations with absolute coefficients of ≥ 0.05 were included as reference configurations. To estimate the effect of unlinked quadruple excitations, the Davidson correction,[19] was employed. The niobium atoms were treated with the Stuttgart basis set and had the first 28 electrons replaced with a quasirelativistic ECP. Carbon and nitrogen atoms were treated with Dunning's correlation-consistent valence double-ζ (i.e., cc-pVDZ). Clusters were oriented the same in both programs (Nb′ on the z axis, Nb_3 in the xz plane), however, the C_{2v} point group allows arbitrary assignment of the σ_v and $\sigma_{v'}$ planes, which reverses the assignment of B_1 and B_2 symmetry labels. To make the output of both programs consistent, we have swapped the B_1 and B_2 labels in discussion of the MOLPRO calculations. Geometric, frequency (for the DFT calculations) and energetic data for all species calculated are presented in the supplementary material.[20]

In order to provide the wave function with enough flexibility to accurately correlate the valence electrons, basis functions with an angular momentum quantum number at least one greater than their angular momentum are required. Therefore, the occupied d-orbitals on the niobium atoms suggest that a basis set including f functions will be necessary to correlate these electrons. Therefore single point energy calculations using larger basis sets were undertaken on the neutral and cationic ground states of Nb_3N_2 in order to investigate the effect of basis set on the (adiabatic) ionization potential (IP) prediction. In a multireference study of the low-lying electronic states of NbC,[21] Balasubramanian used a $5s3p3d2f$ basis set for the niobium atom and a $4s4p2d1f$ basis set to describe the carbon atom. Using this as a guide to the quality of basis set required, single point calculations employed Dunning[22] basis sets of increasing quality (cc-pVDZ-aug-cc-pVTZ) on the nitrogen atoms, with the $(10s9p8d2f1g//5s5p4d2f1g)$ basis set used on the niobium atoms.

The full valence active space of Nb_3N_2 and $Nb_3N_2^+$ includes 40 orbitals in C_{2v} symmetry $(16a_1,5a_2,13b_1,6b_2)$. Using this complete active space leads to an excessive number of configuration state functions (CSFs). Therefore, in order to make the calculations tractable, a reduced active space was employed. The niobium $4s$ and $4p$ and nitrogen $1s$ orbitals $(6a_1,1a_2,3b_1,4b_2)$ were considered to be always doubly occupied (closed). The active space of the remaining 26 orbitals was still too large to be tractable so in order to determine the optimal reduced active space, preliminary CASSCF calculations were undertaken with a large active space. Orbitals that were doubly occupied in all configurations were considered closed and high energy orbitals that were not occupied in any configurations were removed from the active space. The resultant active space considered the lowest $9a_1$, $2a_2$, $5b_1$, and $5b_2$ orbitals to be closed and included the next $3a_1$, $2a_2$, $2b_1$, and $3b_2$ orbitals as the active space. 11 electrons (10 in the case of $Nb_3N_2^+$) were placed in the active space. No excitations were allowed from the closed orbitals, however, they were allowed to relax. This approach led to a total of 7000 CSFs being included.

The same 40 orbitals (viz., $16a_1$, $5a_2$, $13b_1$, and $6b_2$) comprise the full valence active space of Nb_3C_2 and $Nb_3C_2^+$ and the niobium $4s$ and $4p$ and carbon $1s$ orbitals $(6a_1,1a_2,3b_1,4b_2)$ were again closed. Preliminary CASSCF calculations undertaken with a large active space resulted in the lowest $9a_1$, $2a_2$, $5b_1$, and $5b_2$ orbitals being closed and included the next $4a_1$, $1a_2$, $2b_1$, and $3b_2$ orbitals as the active space. Nine electrons (eight in the case of $Nb_3C_2^+$) were placed in the active space. No excitations were allowed from the closed orbitals, however, they were allowed to relax. This approach led to a total of 7000 CSFs being included.

III. RESULTS AND DISCUSSION

A. Nb_3N_2

1. Neutral, Nb_3N_2

The B3LYP/srsc ground state was found to be a $^2B_2$ state, however, the geometry and harmonic vibrational frequencies of this state closely match the $^2B_1$ ground state predicted by Yang *et al.*,[10] using the B3P86/Lanl2dz combination. Recalling the arbitrary assignment of B_1 and B_2 symmetry labels, we therefore contend that we have identified the same ground state as the previous study. We calculate the configuration of this state to be

$$1a_1^2 \cdots 11a_1^2 1b_1^2 \cdots 6b_1^2 1b_2^2 \cdots 6b_2^2 7b_2^1 1a_2^2 \cdots 3a_2^2.$$

The CASSCF ground state is predicted to be a $^2B_2$ state with a doubly bridging geometry, the leading configuration of this state agrees with the B3LYP configuration. The MRCI wave function of the $^2B_2$ state is

$$(63\%|1a_1^2 \cdots 11a_1^2 1b_1^2 \cdots 6b_1^2 1b_2^2 \cdots 6b_2^2 7b_2^1 1a_2^2 \cdots 3a_2^2\rangle$$
$$+ 2.2\%|1a_1^2 \cdots 12a_1^2 1b_1^2 \cdots 6b_1^2 1b_2^2 \cdots 6b_2^2 7b_2^1 1a_2^2 3a_2^2\rangle$$
$$+ 1.9\%|1a_1^2 \cdots 10a_1^2 12a_1^2 1b_1^2 \cdots 6b_1^2 1b_2^2 \cdots 6b_2^2 7b_2^1 1a_2^2 \cdots 3a_2^2\rangle$$
$$+ 1\%|1a_1^2 \cdots 11a_1^2 1b_1^2 \cdots 6b_1^2 1b_2^2 \cdots 5b_2^2 7b_2^1 8b_2^1 1a_2^2 \cdots 3a_2^2\rangle$$
$$+ 1\%|1a_1^2 \cdots 10a_1^2 11a_1^1 12a_1^1 1b_1^2 \cdots 6b_1^2 1b_2^2 \cdots 6b_2^2 7b_2^1 1a_2^2 2a_2^1 3a_2^1\rangle).$$

For the excited states, the B3LYP calculations produce the same approximate order of states as the CASSCF and MRCI calculations, with a large ΔE separating the first excited state from the ground state. At the B3LYP level, three states ($^2A_1$, $^4B_2$, and $^4B_1$) lie 0.64–0.94 eV above the ground state. At the CASSCF level, the first three excited states ($^2A_1$, $^4B_2$, and $^2A_2$) all lie $1.0 \leq \Delta E \leq 1.2$ eV above the ground state energy. However, at the MRCI level, the $^2A_1$ and $^2A_2$ states rise sharply in energy, with only the $^4B_2$ state possessing a ΔE less than 2 eV at the MRCI and MRCI+Q levels. Therefore the $^4B_2$ state can be considered as the first excited state. The leading configuration of this state is generated from the leading configuration of the $^2B_2$ ground state by exciting an electron from the $11a_1$ orbital into $12a_1$ and makes up only 54% of the MRCI wave function for this state,

$$(54\%|1a_1^2 \cdots 10a_1^2 11a_1^1 12a_1^1 1b_1^2 \cdots 6b_1^2 1b_2^2 \cdots 6b_2^2 7b_2^1 1a_2^2 \cdots 3a_2^2\rangle$$
$$+ 6.5\%|1a_1^2 \cdots 11a_1^2 1b_1^2 \cdots 6b_1^2 1b_2^2 \cdots 6b_2^2 7b_2^1 1a_2^2 2a_2^2 3a_2^1 4a_2^1\rangle$$
$$+ 4.3\%|1a_1^2 \cdots 10a_1^2 11a_1^1 12a_1^1 1b_1^2 \cdots 6b_1^2 1b_2^2 \cdots 6b_2^2 7b_2^1 1a_2^2 3a_2^2\rangle$$
$$+ 1.3\%|1a_1^2 \cdots 11a_1^2 1b_1^2 \cdots 6b_1^2 1b_2^2 \cdots 5b_2^2 6b_2^1 7b_2^1 8b_2^1 1a_2^2 \cdots 3a_2^2\rangle$$
$$+ 1.2\%|1a_1^2 \cdots 10a_1^2 11a_1^1 12a_1^1 1b_1^2 \cdots 6b_1^2 1b_2^2 \cdots 5b_2^2 7b_2^1 8b_2^2 1a_2^2 \cdots 3a_2^2\rangle).$$

The leading configuration of the MRCI wave function is quite different from the B3LYP configuration of the same state: $1a_1^2 \cdots 11a_1^2 12a_1^1 1b_1^2 \cdots 6b_1^2 7b_1^1 1b_2^2 \cdots 6b_2^2 1a_2^2 2a_2^2 3a_2^1$ which results from exciting an electron from the $3a_2$ orbital into $12a_1$. This result indicates the degree to which electron correlation influences excited state energies, and demonstrates the requirement for multireference techniques to determine these energies.

Over all multiplicities considered, the DFT calculations predict ΔE figures within a smaller range than that of the CASSCF calculations (2.75 versus 4.75 eV), this could be partially explained as an artifact of the small restricted active space used permitting only limited excitations from the leading configurations of high-spin states. Other notable features from both levels of theory are that the lowest energy states all have $\phi_{Nb'NbNbN} \approx 90°$ or greater and there are very few triply bridging geometries predicted. The lowest energy triply bridging state at the B3LYP/srsc level is the $^4A_1$ state, some 1.16 eV above the ground state. At the CASSCF level the $^8A_2$, $^4B_1$, and $^2B_1$ are the only states possessing triply bridging geometries.

2. Cation, $Nb_3N_2^+$

The ground state of $Nb_3N_2^+$ predicted by B3LYP/srsc is the $^1A_1$ state. The geometry of this state is in agreement with Yang *et al.* as are the harmonic vibrational frequencies. Our calculated electronic configuration of this state is $1a_1^2 \cdots 11a_1^2 1b_1^2 \cdots 6b_1^2 1b_2^2 \cdots 6b_2^2 1a_2^2 \cdots 3a_2^2$ which has removed the unpaired $7b_2$ electron from the neutral configuration.

At the CASSCF level of theory, the ground state is predicted to be the $^1A_1$ state and its geometry closely agrees with the DFT geometry. The MRCI wave function of this state is highly multireference with three major configurations,

TABLE I. Ionization potential of Nb_3N_2 calculated using basis sets of increasing quality. All values are in eV. Experimental IP is taken from Ref. 10.

	Calculated transition	IP
srsc (Nb), cc-pVDZ (N)		
MRCI		4.55
MRCI+Q	$^2B_2 \rightarrow {}^1A_1$	4.80
cc-pVTZ (Nb), cc-pVDZ (N)		
MRCI		4.51
MRCI+Q		4.80
cc-pVTZ (Nb), cc-pVTZ (N)		
MRCI		4.51
MRCI+Q		4.80
cc-pVTZ (Nb) aug-cc-pVTZ (N)		
MRCI		4.51
B3LYP/srsc	$^2B_2 \rightarrow {}^1A_1$	5.67
Experiment		5.44

$$(59\%|1a_1^2\cdots 11a_1^2 1b_1^2\cdots 6b_1^2 1b_2^2\cdots 6b_2^2 1a_2^2\cdots 3a_2^2\rangle$$
$$+5\%|1a_1^2\cdots 10a_1^2 1b_1^2\cdots 6b_1^2 1b_2^2\cdots 7b_2^2 1a_2^2\cdots 3a_2^2\rangle$$
$$+2\%|1a_1^2\cdots 11a_1^2 1b_1^2\cdots 6b_1^2 1b_2^2\cdots 6b_2^2 1a_2^2 2a_2^2 4a_2^2\rangle),$$

and several minor configurations resulting from other double excitations from the leading configuration. The leading configuration of this wave function agrees with the B3LYP configuration of the same state.

The assignment of the ground state at the B3LYP level is not unambiguous, with four states having ΔE values of less than 0.55 eV. Two of these are transition states. The two lowest energy excited states are the $^3B_1$ and $^1B_1$ states, having ΔE values of 0.40 and 0.51eV, respectively. Both these states have triply bridging geometries. At the CASSCF and MRCI+Q levels of theory, however, the assignment of the ground state is clear, with the next lowest energy states being the $^3B_2$ and $^1B_2$ states lying at 0.62 and 0.63 eV, respectively. The geometries of these two states are both doubly bridging. The lowest energy triply bridging states are the $^5A_1$ and $^3B_1$ at 1.51 and 1.59 eV, respectively (at CASSCF level).

3. IP calculations

Yang *et al.* recorded the neutral→cation ZEKE spectrum of Nb_3N_2, which showed vibronic structure built upon an assigned origin at 43901.7 $cm^{-1}(5.4431_5$ eV).[10] The origin band is an extremely high precision determination of the adiabatic IP with which we can compare our predicted values. Our IPs are calculated as the ΔE between the respective ground states of the neutral and cation (i.e., are adiabatic IPs) and are presented in Table I. Thus, both DFT and MRCI IPs are calculated as the $^2B_2 \rightarrow {}^1A_1$ transition, which corresponds to removing the unpaired $7b_2$ electron.

Yang *et al.* used their calculated geometries to predict the adiabatic IP for Nb_3N_2.[10] The ADF and DEMON programs [using Becke-Perdew 86 (BP86) and local-spin-density approximation (LSDA) functionals, respectively] both yield IPs of 5.60 eV, an error of only 0.16 eV and similar to our calculated value of 5.67 eV. The B3P86 functional used by Yang *et al.* with the GAUSSIAN94 program predicts an IP of 6.37 eV, almost 1 eV higher than the experimental value. Previous experience in our group, using the B3P86 functional, confirms the tendency of this functional to predict IPs that are 0.3–1.0 eV higher than experimentally measured values.[23–25]

Using the smallest basis set combination at the MRCI and MRCI+Q levels, the predicted IPs of 4.55 and 4.80 eV, respectively, are substantially below the experimental value. The addition of unlinked quadruple excitations increased the calculated IP value by 0.25 eV; however the resultant value is still ≈0.6 eV below the experimental value. Increasing the basis set on niobium atoms to cc-pVTZ, lowered the MRCI IP slightly to 4.51 eV; however the MRCI+Q IP remained the same (to 3 s.f.). Increasing the basis set quality on the nitrogen atoms did not affect the calculated IPs.

The poor prediction of IP by multireference methods is consistent with previous work. Balasubramanian's study of the Nb_3 cluster predicts the IP of Nb_3 to be 4.50 eV at the MRCI level of theory, using a $(5s5p4d//5s3p2d)$ basis set, inclusion of unlinked quadruples (MRCI+Q) improves this result to 5.09 eV.[1] Single point energies using a larger $(6s6p5d1f//6s4p4d1f)$ basis predict IPs of 5.42 eV and 5.61 eV at the MRCI and MRCI+Q levels of theory, respectively. These values all fall short of the experimental value measured by Knickelbein and Yang[26] of 5.81 ± 0.05 eV.

B. Nb_3C_2

1. Neutral, Nb_3C_2

Unlike Nb_3N_2, Nb_3C_2 has low energy doubly and triply bound structures. Triply bound structures possess $\phi_{Nb'NbNbC} \leq 75°$ and approximately equal Nb–C and Nb′–C bond lengths. The B3LYP/srsc global minimum was found to be a triply bridging structure of $^2B_2$ electronic symmetry. The geometry of this state agrees very closely with the geometry presented by Yang *et al.* for their $^2A_1$ global minimum. Searching for a triply bridging $^2A_1$ state uncovered a transition state, whose geometry differs from the $^2B_2$ state by having one short and two long Nb–Nb bonds (i.e., $\theta_{NbNb'Nb} < 60°$). The energies of these two states are separated by only 1×10^{-5} hartree, suggesting that they represent Jahn–Teller components of a distorted D_{3h} structure. The DFT calculations of Yang *et al.* identified the global minimum as a structure having a $\theta_{NbNb'Nb} > 60°$ using GAUSSIAN94 and DEMON, but ADF predicted a $\theta_{NbNb'Nb} < 60°$. Their attempts to locate both structures (i.e., $\theta_{NbNb'Nb} > 60°$ and $\theta_{NbNb'Nb} < 60°$) within the one program yielded several transition states all below the energy of their D_{3h} structure but no alternate minima.

The B3LYP/srsc wave function of the $^2B_2$ global minimum is

$$1a_1\cdots 11a_1^2 1b_1^2\cdots 6b_1^2 1b_2^2\cdots 6b_2^2 7b_2^1 1a_2^2 2a_2^2,$$

and the wave function of the triply bridging $^2A_1$ state was found to be

$$1a_1 \cdots 11a_1^2 12a_1^1 1b_1^2 \cdots 6b_1^2 1b_2^2 \cdots 6b_2^2 1a_2^2 2a_2^2.$$

Inspection of the $12a_1$ and $7b_2$ orbitals showed both to be comprised of niobium $5s$ and $4d_{z^2}$ orbitals and to have almost identical eigenvalues of $-0.130\,39$ and $-0.130\,35$ a.u., respectively. We therefore consider both the $^2B_2$ and $^2A_1$ states to result from an electron being placed in a formerly degenerate e' orbital (in D_{3h} symmetry). The harmonic frequencies of these states are very similar, further supporting this assertion. The lowest frequency of each state (33 and $25i$ cm^{-1}, respectively) indicates the "softness" of the potential. The DFT calculations used a pruned (75 302) grid and the low frequency modes may shift if a larger grid was used. Repetition of the doublet calculations using the B3P86/Lanl2dz combination (as employed by Yang *et al.*) similarly uncovered almost degenerate $^2B_2$ and $^2A_1$ triply bridging states with very similar geometries to the B3LYP/srsc states. However, the lowest vibrational frequencies of these states are 81 and $80i$ cm^{-1}, respectively, the former being almost identical to that presented by Yang *et al.*

As in the previous calculations of Yang *et al.*, we find near-degenerate doubly and triply bridging structures. The doubly bridging $^2A_1$ structure was found to be a minimum and lies 0.08 eV above the $^2B_2$ global minimum, which is comparable with the ΔE of 0.02 eV quoted by Yang *et al.* The configuration of this state is

$$1a_1 \cdots 10a_1^2 11a_1^1 1b_1^2 \cdots 6b_1^2 1b_2^2 \cdots 6b_2^2 1a_2^2 \cdots 3a_2^2,$$

i.e., an electron pair has moved from the $12a_1$ to the $3a_2$ orbital. Additional doublet states of $^2A_2$ and $^2B_1$ symmetries were found to lie at 0.29 and 0.32 eV, respectively; however, both of these are transition states. The lowest energy quartet was found to be the $^4B_1$ state, with a geometry intermediate between doubly and triply bridging structures. This state is a minimum and was found to be only 0.23 eV above the global minimum. All other quartets were found to be ≥ 0.5 eV above the doublet states and all are transition states. Sextet and octet states were universally high in energy, with the ΔE of sextet states ranging from 1.55 to 1.86 eV and octet states having ΔE values of 2.44–2.99 eV.

The triply bridging $^2A_1$ state is predicted to be the global minimum by all multireference methods employed. A triply bridging $^2B_2$ state is predicted to be near degenerate with the $^2A_1$ ground state, being only 0.05 higher in energy at the CASSCF level and 0.1 eV higher at the MRCI+Q level. As in the DFT calculations, we therefore consider these two states to be components of a Jahn–Teller distorted D_{3h} structure. The MRCI wave function of the triply bridging $^2A_1$ state has three dominant configurations:

$$(68\%|1a_1^2 \cdots 11a_1^2 12a_1^1 1b_1^2 \cdots 6b_1^2 1b_2^2 \cdots 6b_2^2 1a_2^2 2a_2^2\rangle$$
$$+ 1.6\%|1a_1^2 \cdots 10a_1^2 12a_1^1 1b_1^2 \cdots 6b_1^2 1b_2^2 \cdots 6b_2^2 8b_2^2 1a_2^2 2a_2^2\rangle$$
$$+ 1.4\%|1a_1^2 \cdots 11a_1^2 12a_1^1 1b_1^2 \cdots 6b_1^2 1b_2^2 \cdots 5b_2^2 7b_2^2 1a_2^2 2a_2^2\rangle).$$

The wave function of the $^2B_2$ state has four dominant configurations, the last of which has three unpaired electrons,

$$(67\%|1a_1^2 \cdots 11a_1^2 1b_1^2 \cdots 6b_1^2 1b_2^2 \cdots 6b_2^2 7b_2^1 1a_2^2 2a_2^2\rangle$$
$$+ 1.2\%|1a_1 \cdots 10a_1^2 12a_1^2 1b_1^2 \cdots 6b_1^2 1b_2^2 \cdots 6b_2^2 7b_2^1 1a_2^2 2a_2^2\rangle$$
$$+ 1.1\%|1a_1^2 \cdots 11a_1^2 1b_1^2 \cdots 6b_1^2 1b_2^2 \cdots 5b_2^2 7b_2^1 8b_2^2 1a_2^2 2a_2^2\rangle$$
$$+ 1\%|1a_1 \cdots 9a_1^2 10a_1^1 11a_1^2 13a_1^1 1b_1^2 \cdots 6b_1^2 1b_2^2 \cdots 6b_2^2 7b_2^1 1a_2^2 2a_2^2\rangle).$$

Doubly bridging structures were located for $^2A_1$, $^2A_2$, and $^2B_1$ states. The doubly bridging $^2A_1$ structure is 1.05 eV above the ground state at the CASSCF level; however at the MRCI level, the relative energy drops to 0.49 eV and at the MRCI+Q level it is only 0.29 eV above the ground state. The doubly bridging $^2A_1$ state has only two dominant configurations:

$$(67\%|1a_1^2 \cdots 10a_1^2 11a_1^1 1b_1^2 \cdots 6b_1^2 1b_2^2 \cdots 6b_2^2 1a_2^2 \cdots 3a_2^2\rangle$$
$$+ 3\%|1a_1^2 \cdots 9a_1^2 11a_1^1 1b_1^2 \cdots 6b_1^2 1b_2^2 \cdots 7b_2^2 1a_2^2 \cdots 3a_2^2\rangle),$$

of which the leading configuration is consistent with that gained by B3LYP. The $^2A_2$ wave function has eight configurations that contribute more than 1% to the total wave function. The contributions of these configurations that represent excitations from the leading configuration raise the energy of this state from 0.07 eV at the CASSCF level to 0.29 and 0.50 eV at MRCI and MRCI+Q levels, respectively. This state is now higher in energy than the $^2A_1$ state. The $^2B_1$ state is even higher in energy at the MRCI and MRCI+Q levels, the leading configuration of the wave function for this state is an excited state, with three unpaired electrons:

$$63\%|1a_1^2 \cdots 10a_1^2 11a_1^1 1b_1^2 \cdots 6b_1^2 1b_2^2 \cdots 6b_2^2 7b_2^1 1a_2^2 2a_2^2 3a_2^1\rangle.$$

Searches for triply bridging $^2A_2$ and $^2B_1$ minima were unsuccessful. Sextet and octet structures were found to lie high in energy at the CASSCF level and were not investigated at the MRCI or MRCI+Q levels of theory.

Both the B3LYP calculations and the CASSCF/MRCI calculations predict a triply bridging $^2A_1$ and $^2B_2$ pair of states of near-degenerate energy. At the B3LYP level, the near degeneracy of these states, combined with the low harmonic frequencies, suggests a three-way symmetric potential energy surface on which the interconversion of equivalent $^2B_2$ minima occurs via equivalent $^2A_1$ transition states. The CASSCF calculations yield similar geometries for the two states and are consistent with this overall picture, although they predict the $^2A_1$ structure ($\theta_{\mathrm{NbNb'Nb}}<60°$) to be the "minimum." All of these calculations support the apparent flatness of the potential energy surface and a low barrier to interconversion of Jahn–Teller distorted D_{3h} structures. This is similar to what has been described recently for Ag_3,[27,28] where the potential features a "moat" surrounding a D_{3h} structure and there is a barrier to pseudorotation around this moat. For Nb_3C_2, the barrier lies between 0.05 and 0.10 eV ($\approx$400–800 cm^{-1}), dependent on the level of theory. It is difficult to extract a meaningful vibrational frequency along this mode, however it is likely that the zero-point energy lies below this level.

2. Cation, $Nb_3C_2^+$

A $^1A_1$ state is predicted to be the ground state at the B3LYP/srsc level of theory. The geometry for this state is in good agreement with the B3P86/Lanl2dz geometry gained by Yang *et al.*, slightly lengthening all bonds (viz., the Nb–Nb bonds are lengthened by 0.03 Å and the Nb–C bonds by 0.01 Å). The harmonic vibrational frequencies are also in good agreement with the B3P86/Lanl2dz results, with the B3LYP/srsc frequencies indicating three degenerate vibrations, supporting an assignment of D_{3h} symmetry. The 232/235 cm^{-1} frequencies are the two components of the degenerate Nb–C asymmetric stretch with e'' symmetry, the 265 cm^{-1} frequencies correspond to components of the Nb–Nb symmetric stretch with e' symmetry and the 531/533 cm^{-1} frequencies represent components of the symmetric Nb–C stretch of e' symmetry. Constraint of the $^1A_1$ geometry to D_{3h} symmetry at the DFT level resulted in a $^1A_1'$ state with the same energy as the $^1A_1(C_{2v})$ state. In D_{3h} symmetry, addition of an electron to form the neutral would populate a degenerate e' orbital resulting in lowered symmetry of the neutral due to Jahn–Teller distortion as discussed earlier (in Sec. III B 1).

The assignment of the $^1A_1$ ground state is unambiguous with no states lying close in energy to the global minimum; the next lowest energy structure being a doubly bridging $^3A_2$ state, 0.70 eV above the ground state. The $^1A_2$ state is also doubly bridging and lies 0.87 eV above the ground state, very close in energy to the doubly bridging $^1A_1$ state. The only other structure with a ΔE below 1 eV is a $^3B_2$ transition state that is 0.98 eV above the ground state. Quintet and septet structures were found to lie 1.67–3.17 eV above the $^1A_1$ ground state.

The CASSCF, MRCI, and MRCI+Q levels of theory similarly predict the ground state to be the $^1A_1$ state. The CASSCF geometry is a triply bridging geometry with a $\theta_{\mathrm{NbNb'Nb}}=58.8°$ with a Nb–Nb bond length of 2.55 Å and two Nb–NB bond lengths of 2.60 Å. The shortening of the Nb–Nb bond, relative to a D_{3h} ideal, also shortens the Nb–C bonds from 2.07 to 2.02 Å. Attempts to converge a D_{3h} geometry were unsuccessful. The distortion of this geometry from ideal D_{3h} symmetry is likely to be an artifact of the restricted active space chosen as the preliminary CASSCF geometry optimization on this state, which closed only the niobium 4*s* and 4*p* and carbon 1*s* orbitals ($6a_1, 1a_2, 4b_1, 3b_2$) yielded a geometry only slightly perturbed from D_{3h}($\theta_{\mathrm{NbNb'Nb}}=60°$, Nb–Nb=Nb–Nb′=2.60 Å, Nb–C=2.05 Å, Nb′–C=2.04 Å). The MRCI wave function of this state is

$$
\begin{aligned}
&(70\%|1a_1^2\cdots 11a_1^2 1b_1^2\cdots 6b_1^2 1b_2^2\cdots 6b_2^2 1a_2^2 2a_2^2\rangle\\
&+1.9\%|1a_1^2\cdots 10a_1^2 12a_1^2 1b_1^2\cdots 6b_1^2 1b_2^2\cdots 6b_2^2 1a_2^2 2a_2^2\rangle\\
&+1\%|1a_1^2\cdots 10a_1^2 11a_1^1 12a_1^1 1b_1^2\cdots 5b_1^2 6b_1^1 7b_1^1 1b_2^2\cdots 6b_2^2 1a_2^2 2a_2^2\rangle\\
&+1\%|1a_1^2\cdots 11a_1^2 1b_1^2\cdots 6b_1^2 7b_1^2 1b_2^2\cdots 6b_2^2 1a_2^2 2a_2^2\rangle\\
&+1\%|1a_1^2\cdots 10a_1^2 11a_1^1 12a_1^1 1b_1^2\cdots 5b_1^2 6b_1^1 7b_1^1 1b_2^2\cdots 6b_2^2 1a_2^2 2a_2^2\rangle).
\end{aligned}
$$

Significantly, no doubly bridging geometry could be found for this state, all attempts converged to the triply bridging geometry already discussed.

3. IP calculations

Yang *et al.* also recorded the neutral→cation ZEKE spectrum of Nb_3C_2. The spectrum has much richer vibronic features than that of Nb_3N_2, built upon an assigned origin at 40639.0 cm^{-1}(5.0386$_2$ eV).[11] Such a rich spectrum is consistent with a significant change in geometry upon ionization as predicted by the DFT calculations of Yang *et al.*, and all calculations presented herein. Adiabatic IPs at the DFT, MRCI, and MRCI+Q levels of theory were calculated using the ground state of the neutral and cation predicted at that level of theory is presented in Table II. As there was no benefit observed by increasing the quality of the basis set for Nb_3N_2, the MRCI values presented are those calculated using the srsc basis on niobium and cc-pVDZ on carbon.

TABLE II. Ionization potential of Nb_3C_2 calculated at the DFT, MRCI, and MRCI+Q levels. All values are in eV. Experimental IP is taken from Ref. 11.

	Calculated transition	IP
srsc (Nb), cc-pVDZ (C)		
MRCI (TB)	$^2A_1 \rightarrow {}^1A_1$	4.56
MRCI+Q		4.69
MRCI (DB)	$^2A_1 \rightarrow {}^3A_2$	4.55
MRCI+Q		5.07
B3LYP/srsc (TB)	$^2B_2 \rightarrow {}^1A_1$	5.13
B3LYP/srsc (DB)	$^2B_2 \rightarrow {}^1A_1$	5.93
B3LYP/srsc (DB)	$^2B_2 \rightarrow {}^3A_2$	5.75
Experiment		5.04

At the DFT level, the ionization transition for the TB structure is calculated as the $^2B_2 \rightarrow {}^1A_1$ transition, which corresponds to removing the electron from the $7b_2$ orbital. The calculated value for this transition is 5.13 eV, which is only 0.09 eV above the experimental value and therefore is an accurate prediction of the IP within the error expected of DFT calculations. The calculations undertaken by Yang *et al.* predict IPs of 5.16 and 5.12 eV using DEMON (LSDA) and ADF (BP86), respectively; however their GAUSSIAN94 (B3P86) prediction is significantly too high at 5.78 eV, as discussed for the Nb_3N_2 IP (in Sec. III A 3).

For the same isomer, the MRCI and MRCI+Q IPs are calculated as the $^2A_1 \rightarrow {}^1A_1$ transition. At the MRCI level, the calculated value is 4.56 eV, which is significantly below the experimental value. Inclusion of quadruple excitations (MRCI+Q) raises the IP to 4.69, still 0.35 eV below the experimental value.

The DFT ionization transition for the DB structure could be calculated as either $^2A_1(\mathrm{DB}) \rightarrow {}^1A_1(\mathrm{DB})$ or $^2A_1(\mathrm{DB}) \rightarrow {}^3A_2$, and therefore the IP is calculated to each state, yielding values of 5.93 and 5.75 eV, respectively. It is clear that neither of these values correspond closely with the experimental value, supporting the previous assignment of a triply bridging structure for both neutral and cationic Nb_3C_2. Yang *et al.* calculated IPs for the DB species of 6.03 and 6.64 eV using ADF (BP86) and GAUSSIAN94 (B3P86), respectively, both of which are $\approx$1 eV above their respective IPs for the TB species, which is consistent with the DFT results reported herein.

At the CASSCF level the only low energy cationic DB structure is the $^3A_2$ structure and therefore the IP is calculated as the difference between the $^2A_1$ (DB) and $^3A_2$ states, yielding values of 4.55 and 5.07 eV at the MRCI and MRCI+Q levels, respectively. For the latter, this close match to experiment only arises because the addition of quadruple excitations stabilizes the neutral while simultaneously destabilizing the cation. All other MRCI and MRCI+Q IPs are significantly below experimental values and therefore this IP can be considered to be fortuitously close to the experimental value.

IV. CONCLUSIONS

We have calculated the neutral and cationic ground states and low-lying excited states for Nb_3N_2 and doubly and TB isomers of Nb_3C_2 using DFT, CASSCF, MRCI, and MRCI+Q levels of theory. The electronic configurations predicted by DFT agree universally with the leading configurations of the MRCI wave functions; however their contribution to the overall wave function is no more than 70%.

Nb_3N_2 was found at all levels of theory to adopt a doubly bridging structure, consistent with previous theoretical and spectroscopic studies.[10] We calculate no low-lying neutral or cationic excited states that would manifest themselves in the previously published ZEKE spectrum.

For Nb_3C_2 the lowest energy structures of the neutral and cation are triply bridging. The neutral state is Jahn–Teller distorted from D_{3h} symmetry, yielding three identical minima (in C_{2v}) separated by identical transition states, with the barrier to pseudorotation calculated to be between 0.05 and 0.1 eV. We have also investigated the DB isomer using multireference methods. The DB structure is calculated to be only 0.29 eV higher than the TB ground state and we calculate the transition to a corresponding DB cation to be of similar energy to the TB transition. It is therefore possible that features from this isomer may appear in the experimental ZEKE spectrum. Although, the ZEKE spectrum of Nb_3C_2 was scanned to only 500 cm^{-1} above the origin,[11] there were several features in the spectrum which were unassigned by Yang *et al.*, which may be due to the DB isomer.

In the calculation of IPs, while no method of theory used in this study attains consistent "chemical accuracy," it is clear that DFT provides far more accurate IPs than the MRCI calculations, despite being three orders of magnitude faster. Adding quadruple excitations to the MRCI calculations increased IPs by 0.13–0.29 eV, suggesting that inclusion of only single and double excitations is (still!) inadequate to fully describe these systems. Thus it appears that the DFT treatment of correlation effects, while approximate and not systematically improvable, is superior than what can be reasonably produced employing MRCI methods.

ACKNOWLEDGMENTS

We thank Professor Peter Gill for insightful discussions. We are also grateful to the eResearch SA and the National Computational Infrastructure (NCI) facility for computer time.

[1] D. Majumdar and K. Balasubramanian, J. Chem. Phys. **119**, 12866 (2003).
[2] D. Majumdar and K. Balasubramanian, J. Chem. Phys. **121**, 4014 (2004).
[3] D. Majumdar and K. Balasubramanian, J. Chem. Phys. **115**, 885 (2001).
[4] R. Guo and K. Balasubramanian, J. Chem. Phys. **118**, 142 (2003).
[5] K. Das and K. Balasubramanian, J. Chem. Phys. **93**, 625 (1990).
[6] D. Dai and K. Balasubramanian, Chem. Phys. Lett. **195**, 207 (1992).
[7] K. Balasubramanian, J. Chem. Phys. **91**, 307 (1989).
[8] K. Balasubramanian and M. Z. Liao, Chem. Phys. **127**, 313 (1988).
[9] D. S. Yang and P. A. Hackett, J. Electron Spectrosc. Relat. Phenom. **106**, 153 (2000).
[10] D.-S. Yang, M. Z. Zgierski, A. Bérces, P. A. Hackett, A. Martinez, and D. R. Salahub, Chem. Phys. Lett. **277**, 71 (1997).
[11] D.-S. Yang, M. Z. Zgierski, A. Bérces, P. A. Hackett, A. Martinez, D. R. Salahub, P.-N. Roy, T. Carrington, Jr., R. Fournier, T. Pang, and C. Chen,

J. Chem. Phys. **105**, 10663 (1996).
[12] M. J. Frisch, G. W. Trucks, H. B. Schlegel *et al.*, GAUSSIAN 03, Revision D.01., Gaussian, Inc., Pittsburgh, PA, 2004.
[13] P. J. Stephens, F. J. Devlin, C. F. Chabalowski, and M. J. Frisch, J. Phys. Chem. **98**, 11623 (1994).
[14] T. H. Dunning, Jr. and P. J. Hay, in *Modern Theoretical Chemistry*, edited by H. F. Schaefer III (Plenum, New York, 1976), Vol. 3, p. 1.
[15] P. J. Knowles and H.-J. Werner, J. Chem. Phys. **82**, 5053 (1985).
[16] P. J. Knowles and H.-J. Werner, Chem. Phys. Lett. **115**, 259 (1985).
[17] P. J. Knowles and H.-J. Werner, J. Chem. Phys. **89**, 5803 (1988).
[18] P. J. Knowles and H.-J. Werner, Chem. Phys. Lett. **145**, 514 (1988).
[19] S. R. Langhoff and E. R. Davidson, Int. J. Quantum Chem. **8**, 61 (1974).
[20] See EPAPS Document No. E-JCPSA6-130-028917 for energetic and structural information of each respective cluster. For more information on EPAPS, see http://www.aip.org/pubservs/epaps.html.
[21] P. A. Denis and K. Balasubramanian, J. Chem. Phys. **123**, 054318 (2005).
[22] T. H. Dunning, Jr., J. Chem. Phys. **90**, 1007 (1989).
[23] V. Dryza, M. A. Addicoat, J. R. Gascooke, M. A. Buntine, and G. F. Metha, J. Phys. Chem. A **112**, 5582 (2008).
[24] V. Dryza, M. A. Addicoat, J. R. Gascooke, M. A. Buntine, and G. F. Metha, J. Phys. Chem. A **109**, 11180 (2005).
[25] V. Dryza, J. R. Gascooke, M. A. Buntine, and G. F. Metha, Phys. Chem. Chem. Phys. (2008).
[26] M. Knickelbein and S. Yang, J. Chem. Phys. **93**, 5760 (1990).
[27] I. Sioutis, V. L. Stakhursky, R. M. Pitzer, and T. A. Miller, J. Chem. Phys. **126**, 124308 (2007).
[28] I. Sioutis, V. L. Stakhursky, R. M. Pitzer, and T. A. Miller, J. Chem. Phys. **126**, 124309 (2007).